Conference Paper, Published Version

Shimosako, Kenichiro; Suzuki, Kojiro; Tsuruta, Naoki; Tanaka, Tsutomu

Impulsive Breaking Wave Pressure Acting on Seawall Installed on Steep Slope Seabed and the Measures

Coastal Structures 2019 - Nils Goseberg, Torsten Schlurmann (eds) - © 2019 Bundesanstalt für Wasserbau
ISBN 978-3-939230-64-9 (Online) - DOI: 10.18451/978-3-939230-64-9_025

Impulsive Breaking Wave Pressure Acting on Seawall Installed on Steep Slope Seabed and the Measures

K. Shimosako, K. Suzuki, N. Tsuruta & T. Tanaka
Port and Airport Research Institute, Yokosuka, Japan

Abstract: It is well known that the strong impulsive breaking wave pressure acting on the composite breakwater is caused by large rubble mound foundation or steep seabed in front of the breakwater. Such strong wave pressures sometimes induce not only the destruction of structures but also the vibration of the ground and buildings behind the structures. A series of numerical simulation were conducted using the CADMAS-SURF/2D model, that is based on VOF method, to investigate the generation of the impulsive wave pressure acting on the vertical wall on a steep slope. The effect of the large submerged mound in front of the wall in order to reduce the wave force was also examined. It was confirmed that the method of inducing wave breaking by constructing the submerged mound at the offshore side slightly away from the wall is effective. The appropriate position of the submerged mound depends on the tidal level and wave conditions, but it should be installed about one wavelength away from the upright wall.

Keywords: Impulsive breaking wave pressure, Seawall, Steep slope, CADMAS-SURF, Rubble mound

1 Introduction

1.1 Background

The A-coast seawall is constructed on a steep seabed. Since the water depth in front of the seawall is very deep, large waves directly attack the seawall without wave breaking. The seawall was originally covered by wave dissipating blocks to reduce wave overtopping. Recently, new seawall was constructed, and the wave dissipating blocks were removed to improve the landscape since the A-coast is a seaside resort area. However, after construction, strong impulsive breaking wave pressure during typhoon has attacked the seawall, which is supposed to be caused by the rubble mound in front of the seawall. Moreover, this impulsive wave pressure has induced ground and building vibration like an earthquake. To clarify the effect of rubble mound to the impulsive wave pressure and to find countermeasures, a series of numerical calculation were conducted. Especially, large submerged mound cross section that can induce wave breaking and resulting wave energy dissipation were investigated.

1.2 Previous Research

Takahashi et al. (1993) proposed an estimation method to evaluate impulsive breaking wave pressure acting on breakwaters. This estimation method is based on a hydraulic experiment of the breakwater installed on mild slope seabed. Strong impulsive wave pressure in front of the composite breakwater is caused by large rubble mound in front of the caisson according to their experimental results. Just same as the rubble mound, steep seabed was also known to cause the impulsive wave breaking force. To evaluate the impulsive wave pressure on steep seabed, Shimosako et al. (2015) has proposed a new

estimation method using a numerical simulation. We supposed that we can estimate the impulsive wave force at the A-coast seawall. However, there is no method to estimate wave breaking and resulting wave energy dissipation by a countermeasure using much larger rubble mound.

2 Methodology

2.1 Numerical Model

A numerical simulation program using the VOF method, CADMAS-SURF/2D, was used to investigate the impulsive breaking wave pressure acting on seawall. This calculation can reproduce complicated phenomena such as wave breaking, but it is only for fluid without air. In the calculation, rubble mound is treated as porous media conforming to Dupuit-Forchheimer's law. It has been confirmed that the numerical calculation reproduces the wave action properly by comparing with the hydraulic model experiment in advance.

2.2 Cross Sections

Figure 1 shows the typical cross section of seawall at A-coast, which is constructed on the seabed with a steep slope of 1/10, and 8 t armor blocks are placed on the rubble mound consist of 5 to 100 kg stones.

Considering the landscape, the crest height of the armor block is 2 m below L.W.L., not to be seen on the water surface. The design off shore wave height H_0 (return period of 50 years) is 3.6 m and wave period T_0 is 7.2 s.

Ground and building vibration has been induced by impulsive breaking wave when the water level is close to H.W.L. In the present study, we conducted numerical simulations using the regular wave mainly with the wave height of 3.0 m and the wave period of 6.0 s at H.W.L.

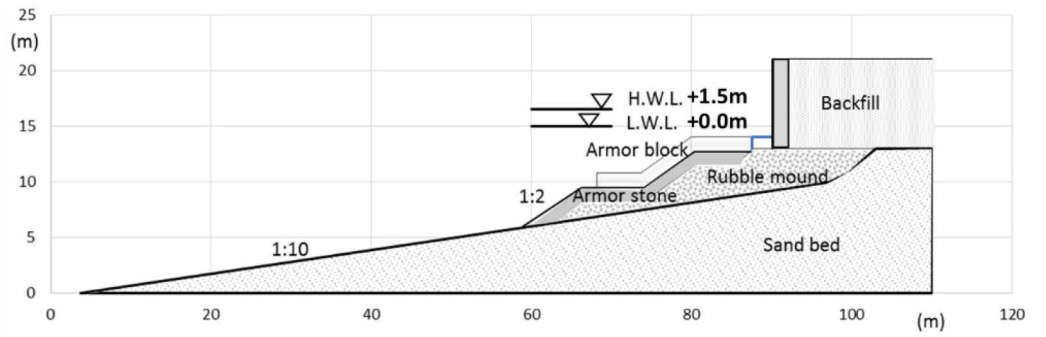

Fig. 1. Typical cross section of seawall at A-coast.

Calculations were carried out in a total of 33 cases in order to investigate the relationship between the generation of impulsive breaking wave and the shape of mound. The crest height from L.W.L. is -6 to +2 m and the width of mound is 2 to 40 m. Calculated condition of the cross sections are summarized in Fig. 2 and Tab. 1.

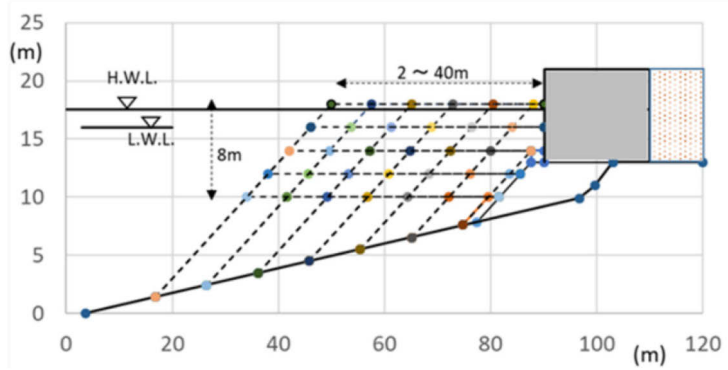

Fig. 2. Calculated condition of cross sections.

Tab. 1. Case number of cross sections.

		Mound crest width(m)						
		47.6	40	32.4	24.8	17.2	9.6	2
Mound crest height from L.W.L.(m)	2		C33	C32	C31	C30	C29	C28
	0		C27	C26	C25	C24	C23	C22
	-2	C21	C20	C19	C18	C17	C16	C15
	-4	C14	C13	C12	C11	C10	C9	C8
	-6	C7	C6	C5	C4	C3	C2	C1

In order to reduce the impulsive wave pressure, modified cross sections (Cdb1 to Cdb5) which have offshore submerged mound shown in Fig.3 were also examined. The crest height of offshore mound is the same as L.W.L. The purpose is to dissipate wave energy by breaking waves on the offshore mound, and also to lower the construction cost by reducing the amount of rubble.

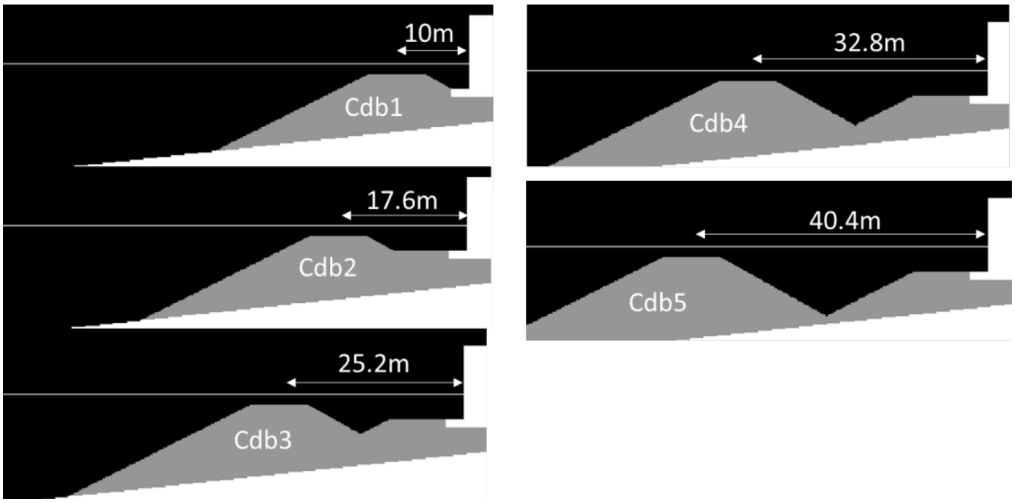

Fig. 3. Modified cross section with submerged mound.

2.3 Calculation Conditions

Figure 4 shows the calculation area with the cross section of C16 that is similar to the actual section of A-coast. The grid size in the horizontal direction Δx is 0.1 m, and in the vertical grid size Δy is 0.2m for the height of 0 to 10 m from the bottom, 0.1 m for 10 to 25 m, and 0.5 m for 25 to 35 m. The water depth at the wave generating-boundary is 17.5 m. The permeability in the mound is assumed to be determined by a small size stone, and the calculations were performed with the diameter of stone being 0.15 m.

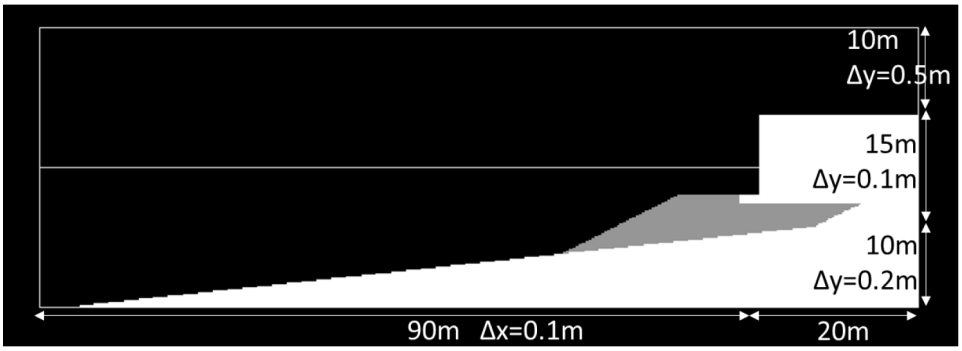

Fig. 4. Calculation area and grid size.

Figure 5 presents a time series of the water surface when the breaking wave collides with the vertical wall in the case of C16. The 1st wave (left) collides immediately after wave breaking (Wagner type breaking), while the 2nd wave (right) collides after wave breaking (Bagnold type breaking).

Figure 6 indicates a time series of the non-dimensional mean wave pressure $p/\rho gH$ of the 1st wave and the 2nd wave for C16. The mean wave pressure is obtained by averaging the wave pressures from the lower end of the upright wall to the water surface in the vertical direction as defined by Eq. (1).

Fig. 5. Water surface profile at wave breaking (C16).

$$\bar{p} = \frac{1}{(\eta - y_{bottom})} \int_{y_{bottom}}^{\eta} p dy \tag{1}$$

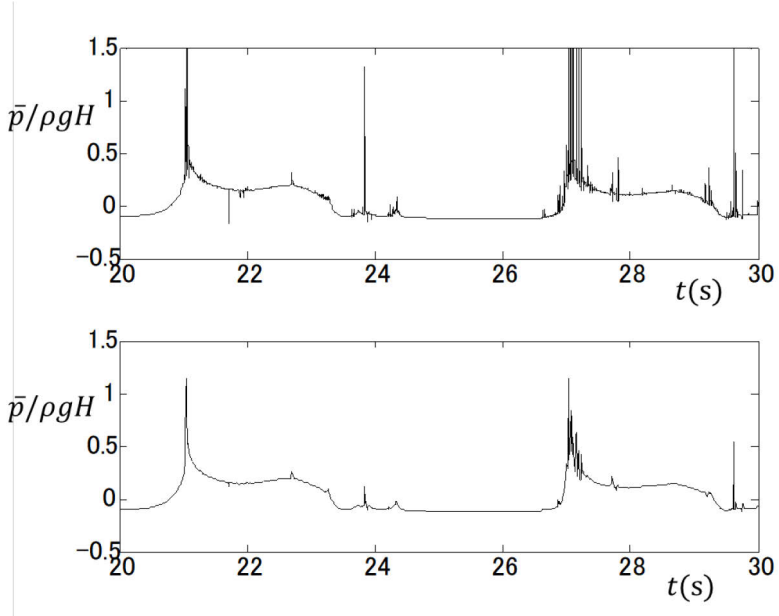

Fig. 6. Example of time series of mean wave pressure.

The calculation is basically performed at a time step of 0.01 s, but for the purpose of satisfying the Courant Condition, it is performed at a smaller time step of around 0.001 s when the impulsive breaking wave occurs. In that case, spike noises different from the actual phenomenon may be generated in the wave pressure (upper figure), so the moving average for 0.01 s are taken to remove such noises (lower figure).

Moreover, in CADMAS-SURF, the donor-acceptor method combining the upwind differencing scheme and the center differencing scheme is used for the calculation of the convection term, and in this study, the calculation was performed under the conditions close to the upwind differencing scheme (VP-DONOR = 0.8).

3 Calculation Results

3.1 Effect of mound height and width

Figure 7 indicates the time series of non-dimensional mean wave pressure $p/\rho gH$ of the 2nd wave in H.W.L. for various mound profile. The impulsive wave pressure is generated in the range enclosed by the solid ellipse including the A-coast mound shape (C16).

In considering the failure of the structure, the impulse (time integral value of wave pressure) is more important than the pressure. Here, the impulse is defined as an integral value of 0.1 s before and 0.15 s after the peak as shown in Fig.8. Figure 9 compares the peak values of non-dimensional pressure and impulse. The maximum wave pressure is generated when the mound crest height is -2 m and the mound width is 17.2 m (C17), while the impulse is maximum when the mound width is 9.6 m (C16).

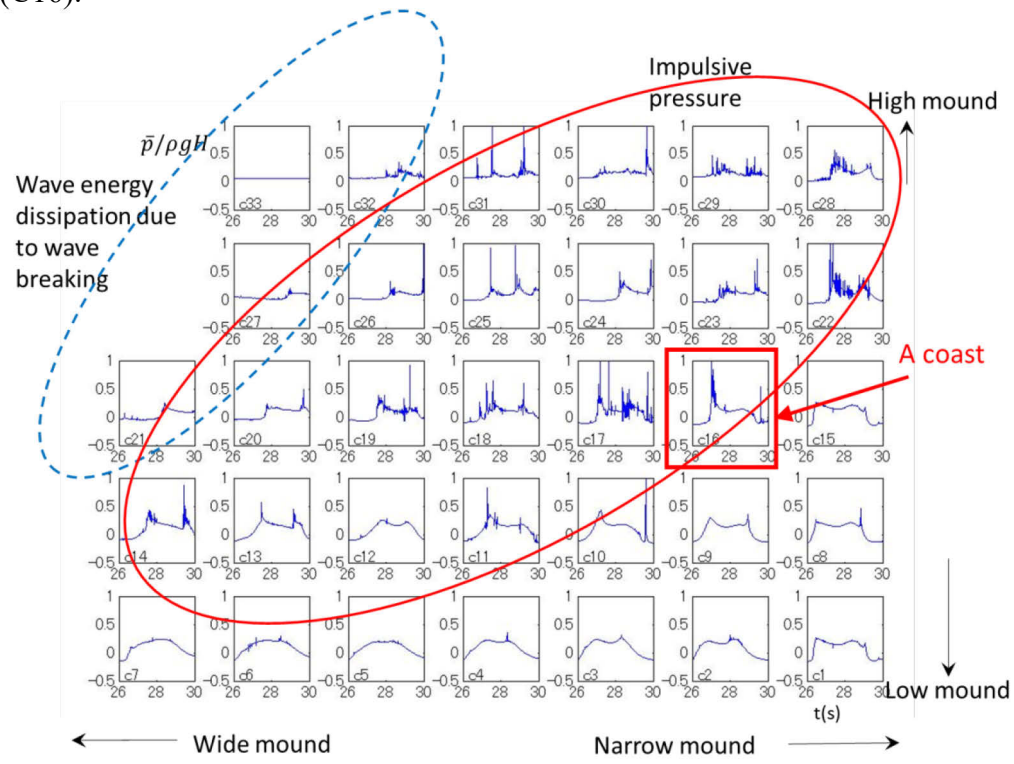

Fig. 7. Time series of mean wave pressure (H.W.L.).

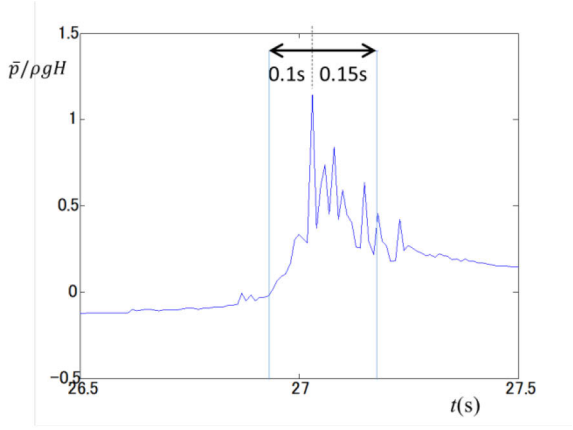

Fig. 8. Definition of impulse.

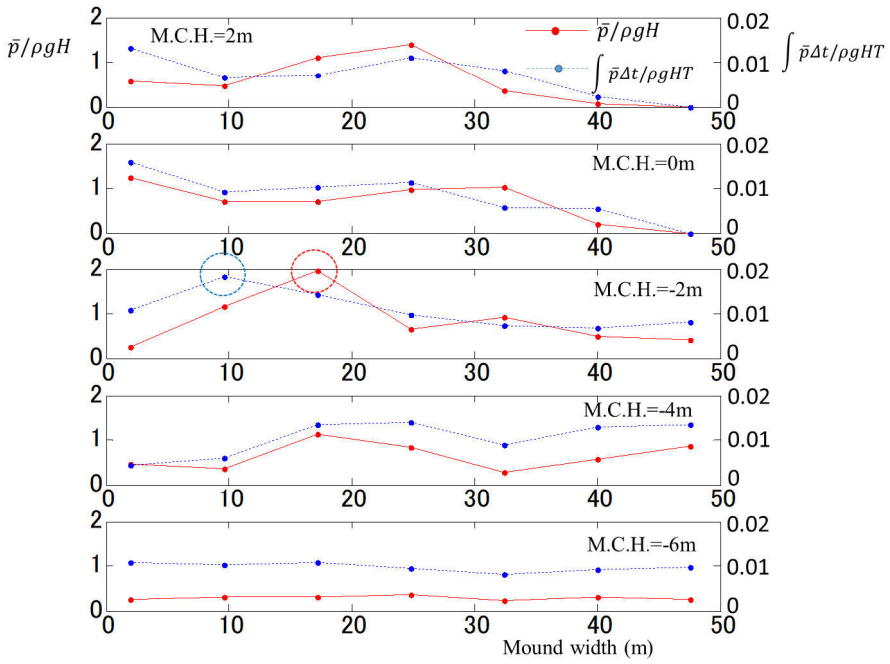

Fig. 9. Peak values of wave pressure and impulse (H.W.L.).

The same time series of mean wave pressure and the peak values of pressure and impulse in L.W.L. are shown in Fig.10 and Fig.11 respectively. The impulsive wave pressure is not generated in relatively low mound condition (C1 to C13) in H.W.L., but it is generated in those condition in L.W.L. The maximum wave pressure is generated when the mound crest height is -2 m and the mound width is 2 m (C15), while the maximum impulse is obtained when the mound crest height is -4 m and the mound width is 2 m (C8).

In L.W.L., when the mound is high and wide, the wave pressure is not large because the wave height becomes small due to the effect of wave breaking. On the other hand, large wave pressure is generated when the mound height and width is relatively small. This is a feature found only seawalls and breakwaters installed on steep bottom slope. In the case of A-coast (C16), the wave pressure is not large in L.W.L., which is consistent with the actual situation.

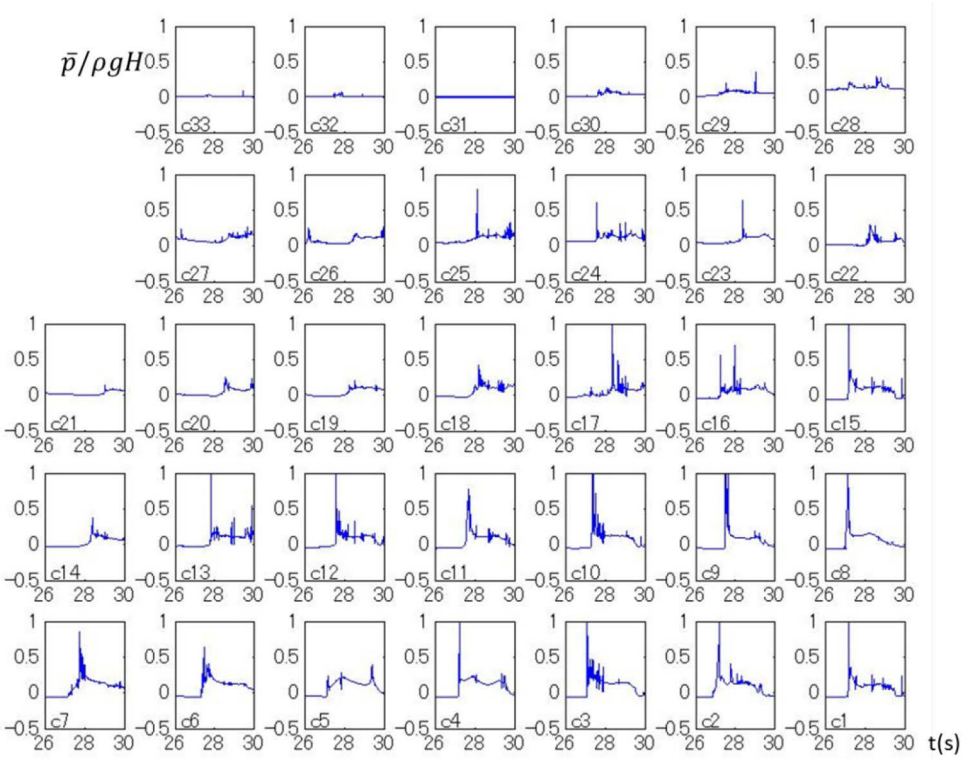

Fig. 10. Time series of mean wave pressure (L.W.L.).

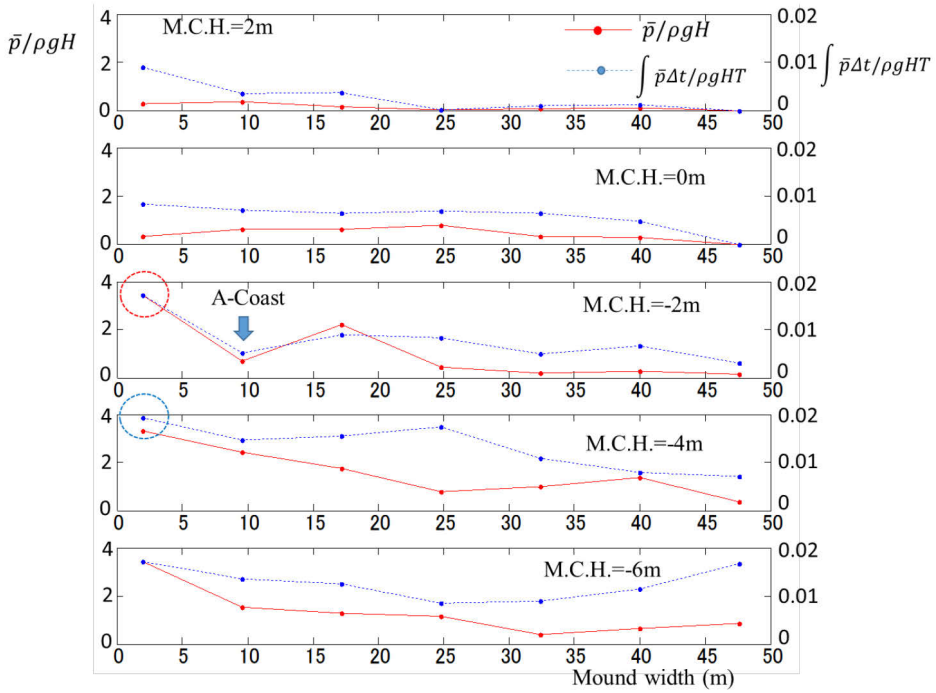

Fig. 11. Peak values of wave pressure and impulse (L.W.L.).

Figure 12 is the same time series of mean wave pressure for various wave periods (4 s, 6 s and 8 s) and wave heights (1 m to 5 m) for the cross section of C17 in H.W.L. As the wave period and wave height increase, the wave force also increases, but when the wave height exceeds 4 m, the force decreases due to the effect of wave breaking.

Figure 13 compares the peak values of pressure and the impulse for the same cases of Fig.12. The wave pressure is maximum when the wave period is 6 s and the wave height is 4 m, while the impulse is maximum when the wave period is 8 s.

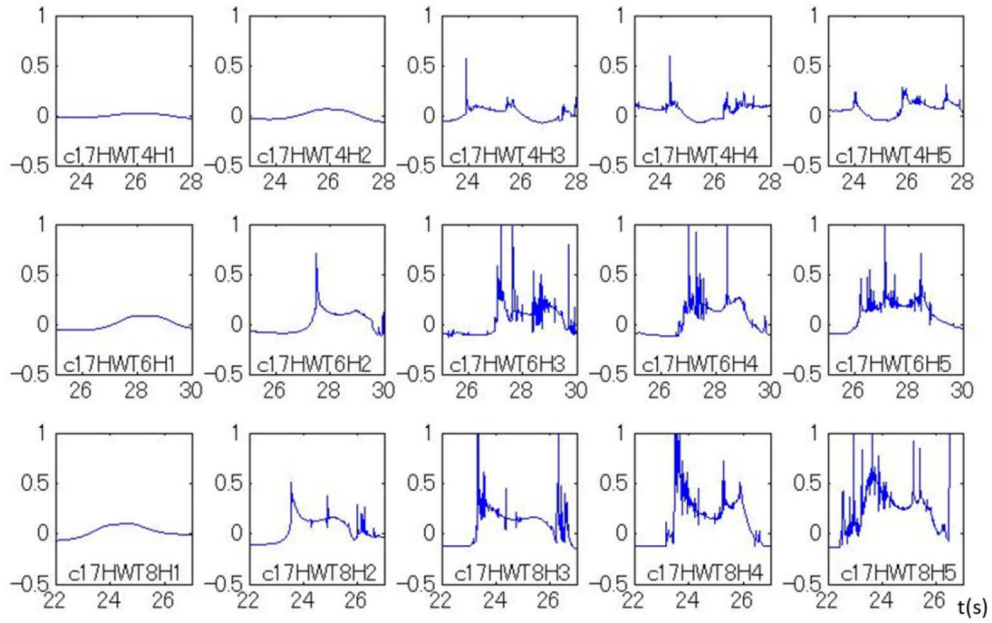

Fig. 12. Time series of mean wave pressure for various wave condition (C17).

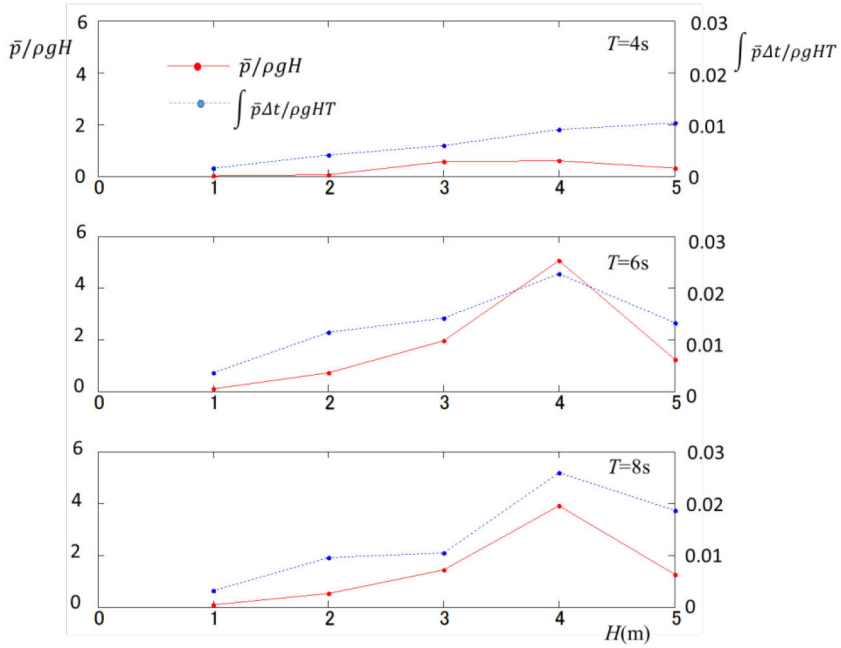

Fig. 13. Peak values of wave pressure and impulse for various wave condition (C17).

3.2 Effect of offshore submerged mound

Figure 14 indicates the time series of the non-dimensional mean wave pressure $p/\rho gH$ of the 2nd wave for modified cross sections. Figure 15 shows the water surface profile at wave breaking. When the position of the offshore submerged mound is close to the seawall (Cdb1), the breaking wave collides directly on the wall and the large impulsive breaking wave pressure is generated. On the other hand, when the offshore mound is relatively far from the seawall (Cdb5), the wave energy is dissipated by wave breaking and then the wave collides the wall. Therefore, the wave pressure is smaller than the other cases.

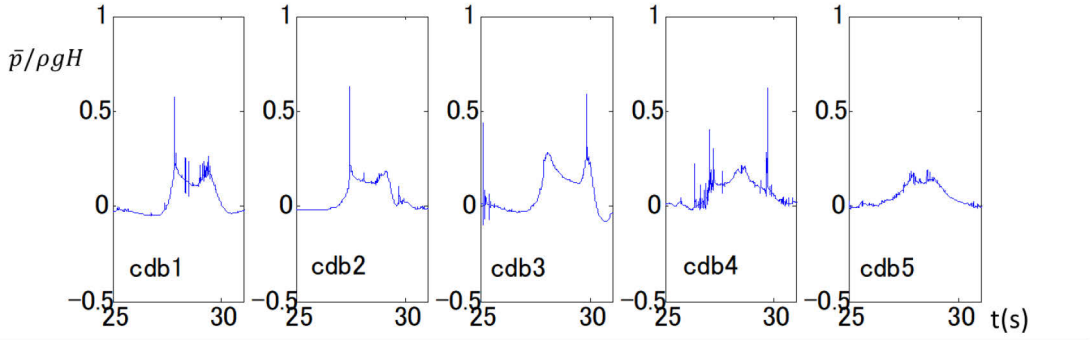

Fig. 14. Time series of mean wave pressure for modified cross sections.

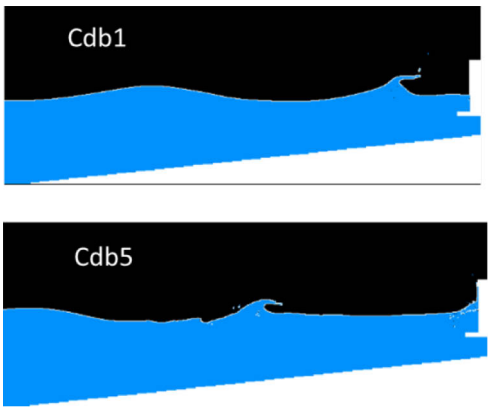

Fig. 15. Water surface profile at wave breaking for modified cross sections.

Figure 16 compares the peak values of pressure and the impulse for the same cases of Fig.14. The peak wave pressure of Cdb5 is much smaller than other cases, while the impulse is small in Cdb4 as well as Cdb5.

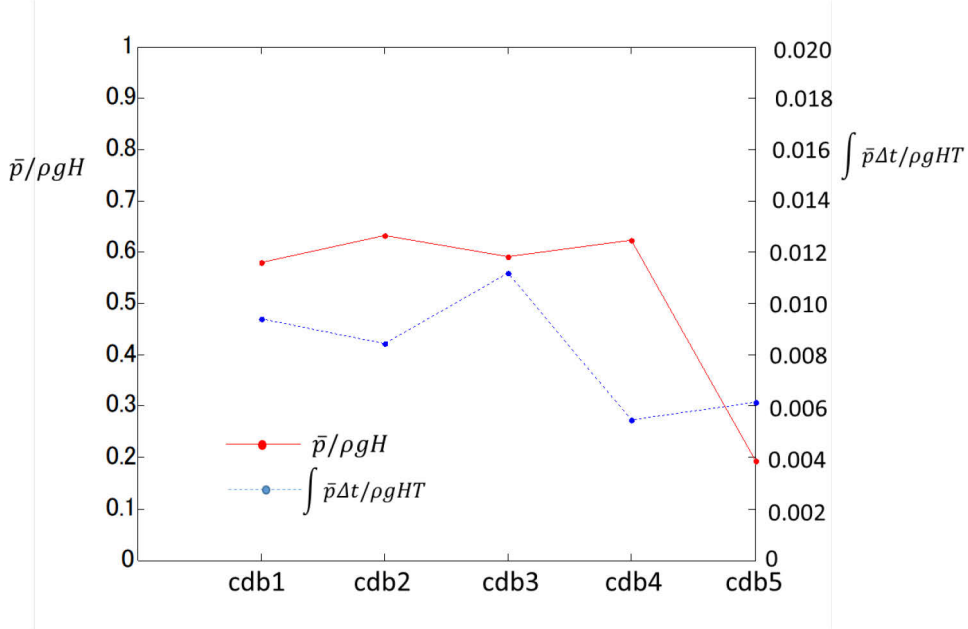

Fig. 16. Peak values of wave pressure and impulse for modified cross sections.

4 Concluding Remarks

A series of numerical simulation were conducted using the CADMAS-SURF/2D to investigate the generation of the impulsive breaking wave pressure acting on the vertical wall on a steep slope, especially the effect of the large submerged mound in front of the wall. In order to prevent the occurrence of impulsive wave pressure, wave dissipating concrete blocks are often installed in front of the vertical wall, but there may be cases where the block cannot be installed due to a landscape problem.

As a countermeasure in such a case, it was confirmed that the method of inducing wave breaking by constructing the submerged mound at the offshore side slightly away from the upright wall in order to reduce the wave force acting on the wall is effective. The appropriate position of the submerged mound depends on the tidal level and wave conditions, but it should be installed about one wavelength away from the upright wall.

In order to clarify the optimum position and cross section of the offshore submerged mound, it is necessary to examine the effect of the height and width of it.

References

Takahashi, S., Tanimoto, K., Shimosako, k., 1993. Experimental Study of Impulsive Pressures on Composite Breakwaters, Report of the Port and Harbour Research Institute, Vol.31, No.5, pp.33-72.

Shimosako, k., Takahashi, S., Tsuruta, N., Suzuki, K., 2015. Estimation of Impulsive Pressure Acting on an Upright Wall on a Steeply Sloping Sea Bottom, in: Proceedings of Coastal Structures 2015.